

Non-Oxidative Mechanisms Are Responsible for the Induction of Mutagenesis by Reduction of Cr(VI) with Cysteine: Role of Ternary DNA Adducts in Cr(III)-Dependent Mutagenesis[†]

Anatoly Zhitkovich,* Yi Song, George Quievryn, and Victoria Voitkun

Brown University, Department of Pathology and Laboratory Medicine, Providence, Rhode Island 02912

Received July 5, 2000; Revised Manuscript Received November 10, 2000

ABSTRACT: Intracellular reduction of carcinogenic Cr(VI) generates Cr–DNA adducts formed through the coordination of Cr(III) to DNA phosphates (phosphotriester-type adduct). Here, we examined the role of Cr(III)–DNA adducts in mutagenesis induced by metabolism of Cr(VI) with cysteine. Reduction of Cr(VI) caused a strong oxidation of 2',7'-dichlorofluorescein (DCFH) and extensive Cr–DNA binding but no DNA breakage. Cr–DNA adducts induced unwinding of supercoiled plasmids and structural distortions in the DNA helix as detected by decreased ethidium bromide binding. Propagation of Cr-treated pSP189 plasmids in human fibroblasts led to a dose-dependent formation of the *supF* mutants and inhibition of replication. Blocking of Cr(III)–DNA binding by occupation of DNA phosphates with Mg²⁺ or by sequestration of Cr(III) by inorganic phosphate or EDTA eliminated mutagenic responses and restored a normal yield of replicated plasmids. Dissociation of Cr(III) from DNA by a phosphate-based reversal procedure returned mutation frequency to background levels. The mutagenic responses at the different phases of the reduction reaction were unrelated to the amount of reduced Cr(VI) but reflected the number and the spectrum of Cr(III)–DNA adducts that were formed. Ternary cysteine–Cr(III)–DNA adducts were approximately 4–5 times more mutagenic than binary Cr(III)–DNA adducts. Although intermediate reaction products (CrV/IV, thiyl radicals) were capable of oxidizing DCFH, they were insufficiently reactive to damage DNA. Single-base substitutions at G/C pairs were the predominant type of Cr-induced mutations. The majority of mutations occurred at the sites where G had adjacent purine in the 3' or 5' position. Overall, our results present the first evidence that Cr(III)–DNA adducts play the dominant role in the mutagenicity caused by the metabolism of Cr(VI) by a biological reducing agent.

Human exposure to hexavalent Cr compounds has been firmly linked with the induction of respiratory cancers (1–3). Industrial exposure to Cr(VI) occurs in several dozens of occupational groups, and there are also concerns about environmental exposure from Cr(VI)-containing waste sites and contaminated water supplies (4). Cr(VI) exists in aqueous solutions as chromate anion that is isosteric with sulfate and phosphate. The structural similarity to these biologically important anions allows rapid uptake of chromate through the general anion channels. Inside the cell, Cr(VI) is reduced to Cr(III) that is the final oxidative form of Cr in all biological systems. This reductive process is believed to be largely nonenzymatic and driven by low molecular weight thiols and ascorbate (5–7). Genetic alterations induced in cells by treatment with Cr(VI) include chromosomal abnormalities and mutations (8–12). The most abundant form of DNA damage produced by exposure of cells to Cr(VI) are ternary complexes of Cr(III) with amino acids and glutathione (13). The predominantly cross-linked amino acids were cysteine (Cys),¹ histidine, and glutamic acid. DNA–

protein and interstrand DNA–DNA cross-links were also detected in exposed cells; however, these lesions are relatively rare (14–16). Ternary DNA–Cr(III)–amino acid adducts are formed through inner-sphere coordination to the oxygen atom of the phosphate group with no evidence for direct binding to bases (17, 18).

Reductive metabolism of Cr(VI) is associated with the production of a variety of intermediate species including Cr(V), Cr(IV), and thiyl and carbon-based radicals (19–21). Oxidation of DNA by these unstable species has been proposed as a potential pathway for the formation of mutagenic damage (22, 23). Another mechanism for the induction of mutagenesis involves the production of Cr(III)–DNA adducts. It has recently been found that ternary DNA adducts formed in the reaction of Cr(III) with glutathione or amino acids were mutagenic in human cells (24). Binary Cr(III)–DNA complexes caused minimal mutagenicity. Cr³⁺ has a complex aqueous chemistry producing an assortment of complexes with water and hydroxyl ions that differ in the reactivity and solubility (25). Given this heterogeneity of Cr(III) complexes, it was important to examine the genotoxic potential of Cr(III)–DNA adducts generated through reduction of Cr(VI). This approach yields the most

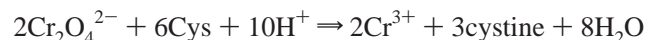
[†] This work was supported by Grant ES 08786 from the National Institute of Environmental Health Sciences.

* Corresponding author: Brown University, Department of Pathology and Laboratory Medicine, Box G–B511, Providence, RI 02912. Telephone: 401-863-2912; fax: 401-863-9008; e-mail: Anatoly_Zhitkovich@brown.edu.

¹ Abbreviations: bp, base pairs; DCFH, 2',7'-dichlorofluorescein; Cys, cysteine.

biologically relevant source of Cr(III) complexes. The relative importance of Cr(III)–DNA adducts in the induction of mutagenic responses by reduction of Cr(VI) has also not been determined.

To address the biological significance of Cr(III)–DNA binding resulting from metabolism of Cr(VI), we examined formation of mutagenic DNA damage during reduction of Cr(VI) by Cys. Among intracellular thiols, Cys has the highest rate of Cr(VI) reduction (5, 7). The stoichiometry of this reaction is described as follows:



Cys and glutathione are probably responsible for the bulk of Cr(VI) reduction in cultured cells since ascorbate is not essential for growth and is typically undetectable in cells *in vitro* (26). On the basis of the relative rates of Cr(VI) reduction (5, 7), Cys is expected to be a predominant reducer when the glutathione-to-Cys ratio is less than 5. CHO cells have been the mostly widely used in the analysis of Cr(VI)-induced DNA damage, and these cells have a ratio of glutathione to Cys of approximately 2:1 (13). We have found that peripheral blood lymphocytes isolated from Cr(VI)-exposed welders had a ratio of about 3:1 indicating that Cys, not glutathione, is likely to be the most important thiol for the metabolism of Cr(VI) in these cells (M. Goulart, G. Quievryn, and A. Zhitkovich, unpublished observations). Recent experiments with animals that were unable to synthesize vitamin C and whose glutathione levels were depleted through pharmacological means suggested that Cys may also play a significant role in metabolism of Cr(VI) *in vivo* (27). Although the role of nonprotein thiols in the reduction of Cr(VI) will be less significant in tissues that are rich in ascorbate (6, 28), Cys still participate in the formation of biologically important coordinate complexes with Cr(III). For example, Cys has been found to be actively cross-linked to chromosomal DNA after exposure of cells to Cr(VI) (13). Formation of these ternary Cys–Cr(III)–DNA adducts represents another mechanism through which Cys could contribute to the induction of genotoxic effects by Cr(VI).

In this work, we have found that Cys-driven metabolism of Cr(VI) led to the formation of DNA damage that was mutagenic during replication in diploid human cells. Ternary cysteine–Cr(III)–DNA and binary Cr(III)–DNA adducts were identified as the principal mutagenic lesions. No DNA damage resulting from oxidative mechanisms was detected despite the formation of a strong fluorescence signal of the oxidant-sensitive probe 2',7'-dichlorofluorescein (DCFH). The results provide the first unambiguous evidence for the critical importance of the Cr(III) pathway in the generation of genotoxic damage arising from the metabolism of carcinogenic Cr(VI) by a biologically relevant reducer.

EXPERIMENTAL PROCEDURES

Materials. Calf thymus DNA (type I) and all reagents for electrophoresis were from Sigma (St. Louis, MO). Chelex-100 resin (200 mesh), Bio-Gel P-30 columns, and cuvettes for electroporation were purchased from Bio-Rad (Hercules, CA). K_2CrO_4 (A.C.S. reagent) was from Aldrich (Milwaukee, WI), 2',7'-dichlorofluorescein diacetate was supplied by Molecular Probes (Eugene, OR). $\text{Na}_2^{51}\text{CrO}_4$ and [^{35}S]-labeled

L-cysteine (without dithiothreitol) were from Amersham (Arlington Heights, IL). Supercoiled and relaxed forms of ΦX174 DNA were obtained from New England Biolabs (Beverly, MA). L-cysteine was from Gibco. The pSP189 plasmid was a gift from Dr. M. Seidman. Large-scale preparations of pSP189 plasmid were done using a kit from Qiagen (Valencia, CA). HF/SV cells were from Dr. H. Ozer. NaOH was used to adjust pH of MOPS buffer. *Caution: Cr(VI) compounds are human carcinogens and appropriate precautions should be taken in handling of these materials.*

Purification of Reagent Solutions. Trace amounts of Fe and Cu were removed from stock solutions of Cys and all buffers by chromatography on Chelex-100 columns. Approximately 0.5 mL of Chelex-100 resin was added to plastic 1-mL columns (Bio-Rad) and then washed with 5 mL of 0.5 M buffer (pH 7.0). The choice of buffer was dictated by the subsequent reaction conditions. Residual buffer was removed from columns by centrifugation at 1000g for 2 min in a swing-bucket rotor. After loading a reagent solution (100 mM Cys or 0.5 M buffer) in a total volume of 0.5 mL, columns were inverted several times and allowed to stand for 10 min at room temperature. Purified solutions were drained from columns by gravity. Neutralization of Chelex resin was critically important for avoiding of oxidation of Cys during purification. Use of unpurified Cys solutions led to a high background mutagenic responses in the absence of Cr(VI). Cys solutions were used within 30 min after purification.

Chromium(VI) Reduction and Oxidation of 2',7'-Dichlorofluorescein (DCFH). Reduction of Cr(VI) was followed by the disappearance of chromate absorbance at 372 nm. The reaction mixture contained 25 mM buffer (pH 7.0), 2 mM Cys, and 50 μM Cr(VI). The reduction process was initiated by the addition of 0.5 mL of 100 μM Cr(VI) solution to 0.5 mL of 2 \times buffer/Cys mixture. Samples were incubated at 37 °C in an electronically controlled cuvette holder of Shimadzu UV1601 spectrophotometer.

Oxidation of DCFH was used as a test for production of oxidants during Cr(VI) reduction. The experimental procedure was adopted from Martin et al. (29) with some modifications. Stock solutions of DCFH-diacetate were prepared in ethanol and stored in small aliquots at –80 °C. Activation of the dye was done by incubation with 10 mM NaOH for 30 min followed by neutralization with 10 vol of 25 mM Chelex-treated sodium phosphate buffer, pH 7.0. A standard reaction mixture contained 10 μM activated DCFH, 25 mM buffer (pH 7.0), 2 mM Cys, and various concentrations of chromate. All reactions were carried out in 96-well plates kept at 37 °C in a SpectraFluor Plus microplate fluorometer (Tecan). Fluorescence was measured with 485-nm excitation and 535-nm emission filters.

DNA Electrophoresis. A standard reaction contained 0.25 μg of plasmid DNA (ΦX174 or pSP189), 2 mM Cys, and various concentrations of Cr(VI) in 25 mM MOPS or sodium phosphate buffer (pH 7.0) in 25 μL volume. Samples were incubated at 37 °C for 60 min and then placed on ice, mixed with 6 \times Ficoll buffer (15% Ficoll 400, 0.25% bromophenol blue, 0.25% xylene cyanol) and loaded onto 1% agarose gels. Electrophoresis was performed in a buffer containing 50 mM Tris-acetate and 1 mM EDTA (pH 8.0). Gels were stained with ethidium bromide, and then photographed under UV illumination using a Bio-Rad GelDoc 2000 documenta-

tion system. Digital images of DNA gels were quantitatively analyzed using Quantity One software (Bio-Rad). Positive controls for DNA strand breakage were generated by incubation of plasmid DNA in 25 mM MOPS buffer (pH 7.0) containing 10 μ M FeCl₃ and 500 μ M ascorbate. Samples were incubated at 37 °C for 60 min followed by the addition of 10 mM EDTA and purification of DNA by the Bio-Gel P-30 chromatography. Digestion of pSP189 DNA with *Eco*RI was done according to the manufacturer's recommendations (New England Biolabs).

Ethidium Bromide Binding Assay. Sheared calf thymus DNA was used in these experiments to avoid confounding effects of unwinding of supercoiled DNA molecules on the extent of ethidium bromide binding. Prior to use, DNA was additionally purified by treatments with RNase A (100 μ g/mL, 37 °C, 60 min) and proteinase K (0.2 mg/mL, 50 °C, overnight) followed by two phenol/chloroform extractions. The reaction mixture contained 1 μ g of DNA, 0–400 μ M K₂CrO₄, 2 mM Cys, and 25 mM MOPS (pH 7.0). A control set of samples additionally contained 5 mM EDTA. The reaction volume was 100 μ L. Samples were incubated for 60 min at 37 °C for 1 h, and then the volume was brought to 200 μ L by the addition of 0.4 M KCl, 5 mM EDTA (final concentrations), and various concentrations of ethidium bromide. Fluorescence measurements were taken following a 10-min incubation at room temperature. To test the presence of potential interactions between Cr(III) and ethidium bromide, we measured fluorescence of the free dye (20 μ M) in samples that contained 2 mM Cys and 0–400 μ M Cr(VI) but lacked DNA. Fluorescence readings were found to be essentially identical in all samples (100–104.3% range relative to control). All fluorescence measurements were obtained using 530-nm excitation and 595-nm emission filters of SpectraFluor Plus microplate fluorometer.

Formation of Cr–DNA Adducts. A standard reaction mixture (final volume = 50 μ L) contained 25 mM MOPS buffer (pH 7.0), 2 mM Cys, 2 μ g of pSP189 DNA, and various concentrations of K₂CrO₄. Samples were incubated at 37 °C for 60 min, and unreacted Cr and Cys were removed by chromatography on Bio-Gel P-30 columns. DNA-containing solutions were supplemented with 200 mM NaCl, and then 2 vol of cold 100% ethanol was added. DNA was precipitated overnight at 4 °C, collected by centrifugation (14000g, 10 min, 4 °C), and then washed 3 times with 70% ethanol. Ethanol precipitation in the presence of 200 mM NaCl removes Cr(III) complexes that are ionically associated with DNA (30). Air-dried DNA pellets were dissolved in sterile deionized H₂O and then used either for cell transfections or quantitation of DNA adducts. Some Cr(VI) treatments of DNA were also performed in 25 mM sodium phosphate buffer (pH 7.0) or in MOPS buffer supplemented with 5 mM EDTA. Blocking of DNA phosphate sites was performed by preincubation of DNA with 10 mM MgCl₂ for 10 min prior to the start of Cr(VI) reduction. Amounts of DNA-bound Cr and Cys were quantified using radiolabeled [⁵¹Cr]Na₂CrO₄ and [³⁵S]L-cysteine, respectively (18).

Dissociation of Cr(III)–DNA Adducts. The formation of Cr–DNA adducts was performed with 50 μ M Cr(VI) in MOPS buffer as described above. Unbound Cr was removed by the Bio-Gel P-30 chromatography followed by the ethanol/NaCl precipitation. Cr-adducted plasmids were dissolved in 50 mM sodium phosphate (pH 7.0) and then

incubated for the different periods of time at 37 °C. Released Cr(III) was removed by a passage through P-30 columns, and purified DNA was assayed for Cr or used for mutagenesis experiments. A control set of Cr-adducted DNA was incubated in 50 mM MOPS (pH 7.0). The amount of DNA-bound Cr was determined using trace amounts of [⁵¹Cr]-labeled chromate.

Shuttle-Vector Mutagenesis. An SV40-based pSP189 plasmid containing the *supF* gene as a mutagenic target was used in shuttle-vector mutagenesis experiments (31). The plasmid contains the SV40 origin of replication and large T-antigen, which permits replication of this plasmid in any human cell line. The presence of a unique 8-bp signature sequence in each individual plasmid molecule allows determination of sibling mutants following sequencing. Replication of the adducted and normal plasmids was performed in human diploid fibroblasts immortalized with SV40 virus (HF/SV cell line). Mutant selections were performed using *Escherichia coli* MBL50 strain (a gift from Dr. C. Pueyo). This indicator *E. coli* strain has two amber mutations suppressed by the *supF* gene: *araC* and *lacZ* (32). Mutation in the *araC* gene allows selection of the colonies with a mutated *supF* gene on media containing L-arabinose. Amber mutation in the *lacZ* gene permits white/blue color screening of colonies. Cr-treated or control plasmids were transfected into the cells using TransFast transfection reagent (Promega) according to manufacturer's recommendations. A morphological assessment of the cells 2–3 days after the transfection indicated that transfection efficiency was close to 100%. Cytotoxicity determined by the number of the detached cells typically was less than 20%. After 42–48 h propagation time, plasmids were recovered from cells by a plasmid isolation kit from Qiagen. DNA was precipitated with ethanol and dissolved in deionized H₂O. Plasmids were electroporated into the indicator bacteria *E. coli* MBL50 according to Hanahan et al. (33). The total number of transformants was determined on the minimal agar plates containing 30 μ g/mL ampicillin and 0.5 μ g/mL chloramphenicol. Mutant selection was performed on plates additionally containing 2 mg/mL L-arabinose. Mutation frequency was calculated as the ratio of ampicillin/arabinose-resistant to ampicillin-resistant colonies in each sample.

Sequencing of Mutants. Mutant colonies were obtained from samples treated with 50 μ M Cr(VI) which typically resulted in at least 10-fold increase in mutation frequency over background. The mutant *E. coli* colonies were inoculated into 2 mL of LB medium containing 50 μ g/mL ampicillin, and the cultures were incubated at 37 °C overnight. Plasmids were isolated as described above, and 0.5–1 μ g of DNA was used in the sequencing reaction. The *supF* gene was sequenced using an ABI Prism 377 DNA Sequencer (Perkin-Elmer). The sequencing primer corresponding to the positions 4889–4908 of the pSP189 plasmid was 5'-GGCGACACGGAATGTTGAA-3'.

RESULTS

Reduction of Cr(VI) and Formation of DCFH-Oxidizing Species. The disappearance of Cr(VI) in the presence of 2 mM Cys exhibited a single component kinetics with half-life of approximately 10 min in MOPS buffer (Figure 1). Reduction of Cr(VI) in MOPS buffer was essentially complete after 60 min. Addition of Mg²⁺ ions had no effect

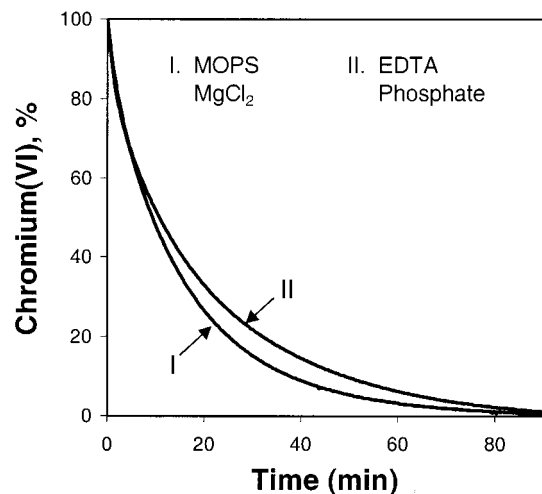


FIGURE 1: Reduction kinetics of chromate in the presence of 2 mM cysteine. Reactions were carried out at 37 °C with 50 μ M chromate in 25 mM sodium phosphate, pH 7.0, and in 25 mM MOPS, pH 7.0, alone or supplemented with 10 mM $MgCl_2$ or 5 mM EDTA.

on the rate of reduction, whereas reactions performed in the presence of 25 mM phosphate or 5 mM EDTA had approximately 20–25% slower reduction rates. The time-course of DCFH oxidation in MOPS buffer by three concentrations of Cr(VI) showed increased production of oxidizing species up to 1 h of incubation (Figure 2, panel A). There was little or no increase in the oxidation of DCFH at later time points, which was consistent with the results of Cr(VI) reduction based on chromate absorbance measurements. The oxidation of DCFH was dose-dependent at different time points examined (Figure 2, panels A and B). Addition of Mg^{2+} ions did not change the extent of DCFH oxidation, whereas EDTA increased the overall level of oxidants (Figure 2, panel B). The oxidation of DCFH by Cr(VI)/Cys mixtures in the phosphate buffer was also higher relative to MOPS, and it was similar to EDTA-containing samples (not shown). The comparison of the rate of chromate reduction and the extent of DCFH oxidation under different buffer conditions points to the inverse relationship between these two parameters; however, additional experimentation is needed to confirm this correlation.

Structural Changes in Cr-Modified DNA. Electrophoretic analysis of plasmid DNA was performed to examine induction of conformational changes and strand breakage following reactions with Cys/Cr(VI) mixtures. Incubation of the pSP189 DNA during reduction of Cr(VI) in MOPS buffer resulted in a slower electrophoretic mobility of adducted plasmids, with particularly noticeable changes for all supercoiled forms (Figure 3, panel A). These differences in electrophoretic mobility were caused by the formation of Cr–DNA adducts since samples containing the Cr(III) chelator EDTA had unaltered mobility of plasmid bands. The comparison between EDTA-containing and EDTA-free reactions also shows that Cr–DNA binding leads to a diminished intensity of ethidium bromide staining. The amount of the monomeric supercoiled DNA (form I) was similar in all samples suggesting a lack of DNA strand breakage. The pSP189 plasmids are typically isolated as a mixture of the supercoiled forms of the monomeric and dimeric molecules (34). Comigration of the dimeric supercoiled form and nicked monomeric molecules leads to difficulties in evaluating the

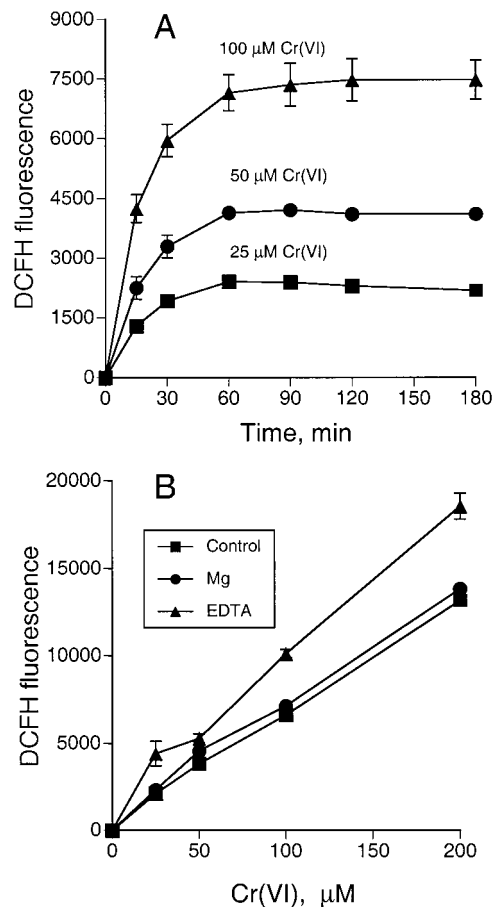


FIGURE 2: Oxidation of DCFH during Cr(VI) reduction with 2 mM cysteine. All reactions were done at 37 °C in 25 mM MOPS, pH 7.0. (A) time-course; (B) influence of Mg ions and EDTA on oxidation of DCFH. Shown are means \pm SD of 3–6 independent measurements. Where not seen, error bars were smaller than the data symbols.

migration properties of relaxed pSP189 molecules. To overcome this problem, we utilized commercial Φ X174 plasmid preparations that contained only monomeric forms (Figure 3, panel B). The amount of nicked plasmid molecules (form II) was similar in all samples demonstrating the absence of DNA strand breakage even at very high Cr(VI) concentrations. The overall decrease in the rate of migration of supercoiled DNA was much greater in comparison to relaxed DNA which could reflect either a much higher number of Cr–DNA adducts or unwinding of supercoiled plasmids. To test whether this was caused by different levels of Cr–DNA binding, we examined formation of Cr–DNA adducts using supercoiled and relaxed forms of Φ X174 DNA. Levels of Cr adducts in relaxed DNA preparations relative to supercoiled DNA formed following incubations with 25, 50, 100, or 200 μ M Cr(VI) were 91.7, 107.1, 99.8, and 93.2%, respectively (mean = $98.0 \pm 6.1\%$). Thus, differences in the electrophoretic mobility of Cr-treated supercoiled and relaxed DNA molecules are caused by a greater sensitivity of the supercoiled DNA conformation to modifications of the phosphate backbone by Cr(III).

Induction of structural changes in Cr-adducted DNA was further investigated by the ethidium bromide-binding assay (35, 36). The amount of DNA-bound ethidium bromide was assessed by the intensity of fluorescence after the direct excitation of the dye molecules at 530 nm. Under these

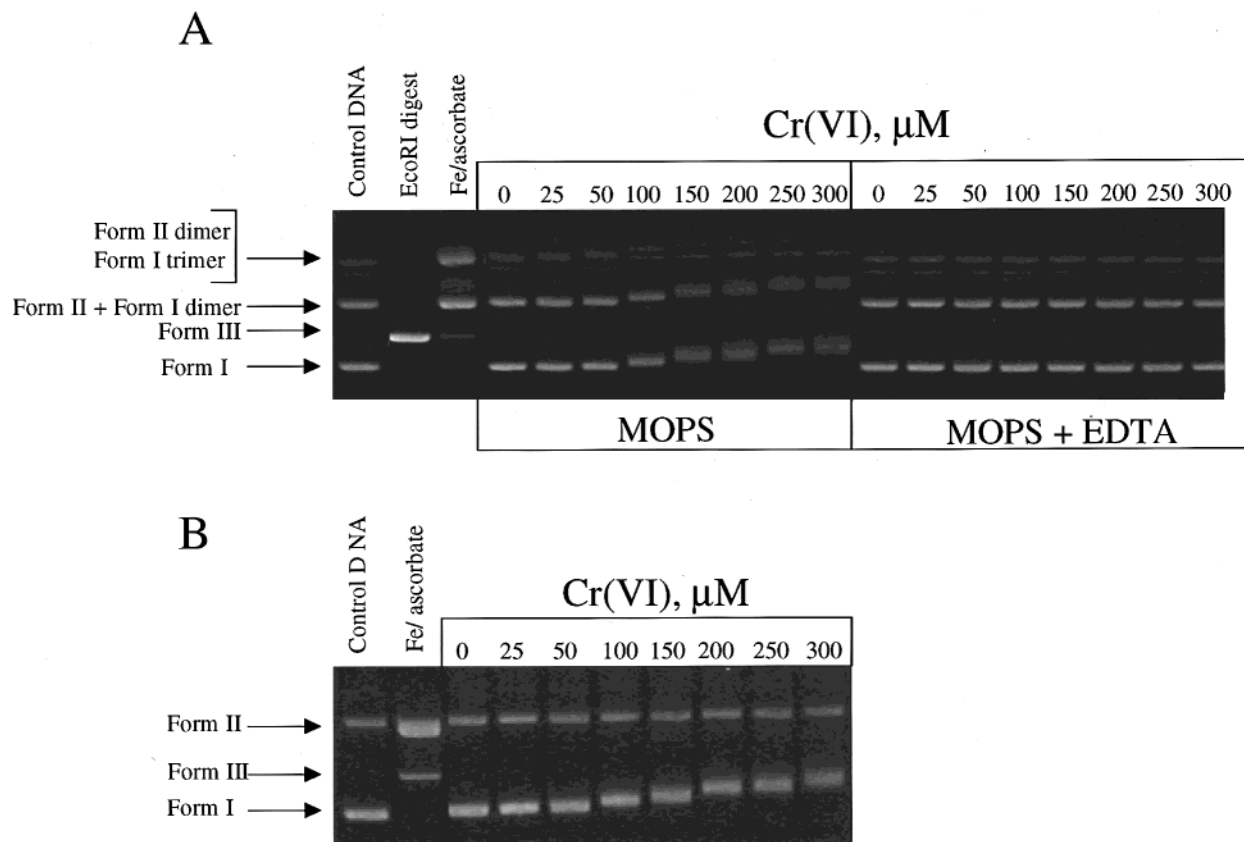


FIGURE 3: Electrophoretic analysis of Cr(VI)-treated plasmid DNA. Each sample contained 25 mM MOPS, pH 7.0, 2 mM cysteine, 0.25 μg of plasmid DNA and various amounts of K_2CrO_4 in a 25 μL volume. A separate set of samples additionally contained 5 mM EDTA. The reaction was performed at 37 $^\circ\text{C}$ for 60 min followed by immediate loading on 1% agarose gels. Fe/ascorbate–DNA was treated with 10 μM FeCl_3 and 500 μM ascorbate to generate nicked plasmids. Form I, intact supercoiled plasmids; form II, open circular plasmids containing one or more single-strand breaks; form III, linearized plasmids. (A) Agarose gels of pSP189 DNA treated with Cr(VI). (B) Agarose gels of ΦX174 DNA treated with Cr(VI).

conditions, changes in fluorescence indicate the presence of structural distortions in DNA caused by chemical modifications (35, 36). Binding of Cr(III) to DNA resulted in a dose-dependent decrease in the fluorescence of ethidium bromide (Figure 4, panels A and B). A statistically lower fluorescence was observed with as low as 50 μM Cr(VI) ($P = 0.0002$, two-sided t -test). The decrease in the amount of DNA-bound ethidium bromide was not caused by different kinetics of binding to DNA since the shapes of the concentration-dependence curves were practically identical for both control and Cr-modified DNA. Blocking of Cr(III)–DNA adduct formation by the inclusion of EDTA in the reduction reactions (see below) resulted in the fluorescence measurements indistinguishable from control. There was no direct interaction between the metal and the ethidium bromide judging by the unaffected fluorescence of the free dye (20 μM) in the presence of 0–400 μM Cr(VI) (see Experimental Procedures). Even samples that contained 20-fold molar excess of Cr over the dye concentration had a normal fluorescence ($101.5 \pm 2.8\%$ relative to control). This finding is in agreement with the absence of any reasonable binding site for Cr(III) in ethidium bromide molecule. Additionally, ethidium bromide is positively charged which would greatly diminish any possible interaction with Cr^{3+} centers. At saturating concentrations of ethidium bromide, the modification of DNA with 400 μM Cr(VI) led to approximately 60–65% decrease in fluorescence relative to control. Treatment of DNA with 200 and 400 μM Cr(VI) resulted in DNA

binding of 0.06 and 0.11 Cr atoms/nucleotide, respectively. At these levels of Cr(III)–DNA adducts, the extent of structural distortions in DNA as determined by the inhibition of ethidium bromide fluorescence appears to be greater than it was reported for cisplatin-modified DNA (35, 36). Incubation of DNA with cisplatin results in the formation of Pt adducts at N-7 positions of dG and dA that cause a variety of structural distortions, including bending and unwinding of the DNA helix (37, 38). These Pt(II)–DNA adducts have been found to be mutagenic (39, 40).

Formation of Cr–DNA Adducts. Formation of Cr(III)–DNA adducts during reduction of Cr(VI) in MOPS buffer showed a linear dose-dependence (Figure 5). Inclusion of EDTA or Mg^{2+} ions in MOPS buffer completely eliminated Cr–DNA binding. EDTA forms a very stable pentacoordinate complex with Cr(III) (41) that would block Cr(III) from binding to DNA. Mg^{2+} binds to DNA phosphates and at 10 mM concentration, all DNA phosphates were found to be occupied by this ion (42). The phosphate group has been previously shown to serve as the principal point of Cr(III) attachment to DNA and mononucleotides (18, 43, 44). Unlike reactions in MOPS buffer, reduction of Cr(VI) in phosphate buffer failed to yield Cr–DNA adducts. Inorganic phosphate forms very stable and usually water-insoluble complexes with Cr(III). We did not observe visible precipitation in the phosphate-containing samples, which was probably due to low concentrations of reagents and small reaction volumes. It is also possible that the bulk of Cr(III) was present in the

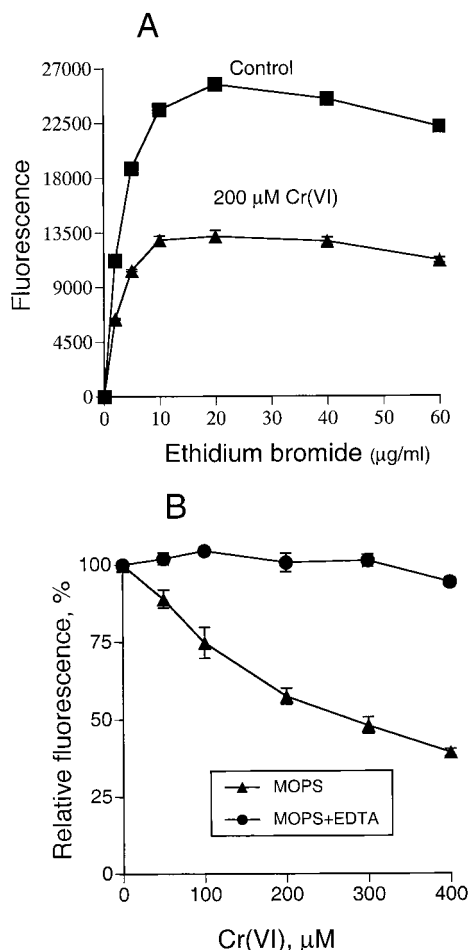


FIGURE 4: Diminished binding of ethidium bromide to Cr-treated DNA. Calf thymus DNA (1 μg) was treated with 0, 50, 100, 200, 300, or 400 μM Cr(VI) in the presence of 2 mM cysteine and 25 mM MOPS, pH 7.0. After 60-min incubation at 37 $^{\circ}\text{C}$, 0.4 M KCl, 5 mM EDTA, and various concentrations of ethidium bromide were added to each sample. Fluorescence was recorded with 530-nm excitation and 595-nm emission filters. (A) Fluorescence of control and Cr-treated DNA in the presence of various concentrations of ethidium bromide. Shown are means of three independent measurements. Error bars are not seen since they are smaller than the data symbols. (B) Fluorescence of DNA treated with various concentrations of Cr(VI). Ethidium bromide was added to the final concentration of 40 $\mu\text{g}/\text{mL}$. Shown are means \pm SD of six independent measurements. MOPS: DNA was treated under the standard conditions in MOPS buffer; MOPS + EDTA: the reactions additionally contained 5 mM EDTA.

form of mixed-ligand complexes that remained in the solution. In addition to phosphate, these Cr(III) complexes would be likely to contain Cys and hydroxyl ions.

Shuttle-Vector Mutagenesis. Mutagenic potential of DNA modifications produced during Cr(VI) reduction was examined using the pSP189 shuttle-vector (31). This plasmid is capable of replicating in human cells, which permits analysis of mutagenic properties of DNA adducts using replication machinery of intact cells. Selection of *supF* mutants was carried out using *E. coli* MBL50 strain and plates containing L-arabinose. DNA damage induced during incubation with Cr(VI)/Cys in MOPS buffer decreased a number of replicated plasmids recoverable from human fibroblasts, as evidenced by a progressively lower yield of ampicillin-resistant colonies in Cr-exposed samples (Figure 6, panel A). Exponential fit of the data gave an $\text{LD}_{50} = 22 \mu\text{M}$ Cr(VI), which corresponds to approximately 5 Cr adducts/1000 bp. DNA samples

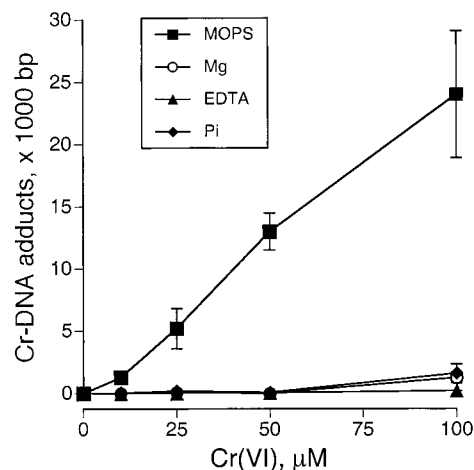


FIGURE 5: Formation of Cr–DNA adducts under different buffer conditions. A standard reaction mixture contained 25 mM buffer, (pH 7.0), 2 mM cysteine, 2 μg of pSP189 DNA, 200000–500000 cpm [^{51}Cr]–chromate and various concentrations of nonradioactive Cr(VI). Reaction volume was 50 μL . All incubations were done at 37 $^{\circ}\text{C}$ for 60 min followed by removal of unbound Cr by Bio-Gel P-30 chromatography and ethanol precipitation. MOPS: the reactions contained MOPS buffer; Mg: MOPS buffer was supplemented with 10 mM Mg^{2+} ; EDTA: MOPS buffer supplemented with 5 mM EDTA; Pi: reaction contained 25 mM sodium phosphate. Shown are means \pm SD from six independent experiments.

containing 25 and more Cr adducts/1000 bp ($> 100 \mu\text{M}$ Cr(VI) exposure) produced no bacterial colonies indicating a complete block of replication of these plasmids in human cells. In contrast, MOPS-based reaction mixtures that contained either Mg^{2+} or EDTA had unaffected yields of transformants in the entire range of Cr(VI) concentrations demonstrating the primary role of Cr(III)–DNA adducts in the replication blockage. Treatment of pSP189 plasmids with Cr(VI) and Cys in MOPS buffer led to the formation of mutagenic DNA damage (Figure 6, panel B). This mutagenic response was linear in the range from 0 to 100 μM Cr(VI) reaching approximately 20-fold increase over background at the highest dose. Blocking Cr–DNA binding by the inclusion of inorganic phosphate, EDTA, or Mg^{2+} ions in the Cr(VI) reaction mixtures eliminated the mutagenic responses at all Cr(VI) concentrations. This finding strongly implicated Cr(III)–DNA adducts as being responsible for the mutagenic effects induced by Cr(VI) metabolism. The template properties of pSP189 DNA treated with Cr(VI)/Cys in the presence of inorganic phosphate were similar to control, as judged by unaffected yields of bacterial transformants. For example, even incubation of DNA with the highest Cr(VI) concentration (200 μM) gave a 98.3% relative transformation efficiency. Importantly, the absence of mutagenic and replication-blocking DNA lesions in samples containing phosphate, EDTA, or Mg^{2+} was not associated with a significantly different kinetics of Cr(VI) reduction (Figure 1) or a decreased production of DCFH-oxidizing species (Figure 2, panel B).

Although three different approaches for blocking of Cr–DNA binding eliminated the mutagenic response, there was still the possibility that the presence of Mg, EDTA, or phosphate somehow perturbed the formation of DNA-reactive products and/or changed DNA structure modifying formation of mutagenic damage through Cr-independent mechanisms. The most rigorous test for the importance of

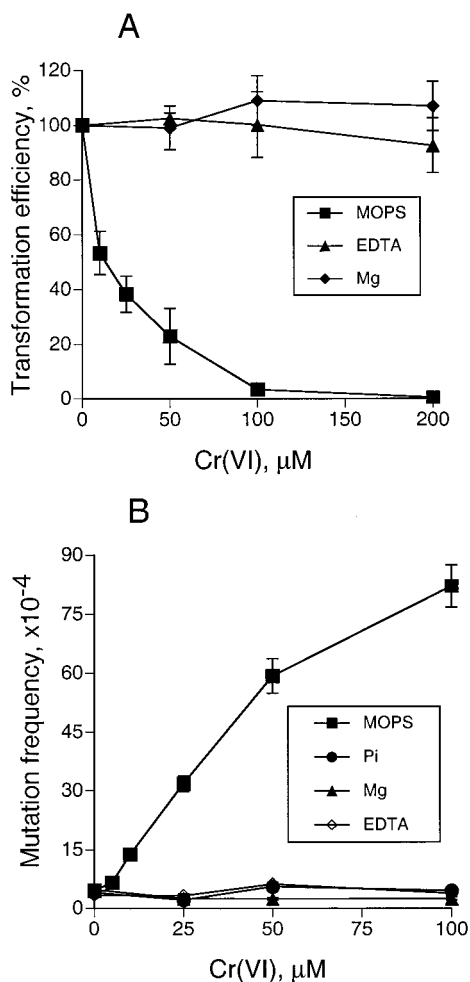


FIGURE 6: Survival and mutagenesis in pSP189 plasmids treated with chromium (VI). DNA was treated with Cr(VI) as described in Figure 5, and then transfected into HF/SV human fibroblasts. After 48 h, plasmids were recovered and electroporated into indicator bacteria to score transformants and arabinose-resistant mutants. Shown are means \pm SD of 6–8 independent experiments. (A) Survival of pSP189 plasmids as measured by the transformation efficiency; (B) mutation frequency.

Cr–DNA adducts in the induction of mutagenesis can be performed by analyzing mutational response before and after stripping of Cr(III) from DNA. We found that incubation of Cr(VI)-treated DNA in 50 mM phosphate (pH 7.0) for 24 h released approximately 85–90% of DNA-bound Cr(III) (Figure 7, panel A). Dissociation of the majority of Cr–DNA adducts by this reversal procedure resulted in almost complete loss of the mutagenic response induced by Cr(VI)/Cys metabolism (Figure 7, panel B). A marginal increase in mutations in phosphate-treated samples over background was probably caused by the residual Cr–DNA adducts (10–15% of the initial amount). The release of Cr(III) from DNA has also increased a relative yield of bacterial transformants from 22.1 ± 12.9 to $81.0 \pm 1.3\%$, demonstrating the loss of the majority of replication-blocking lesions.

Mutagenic Response and Production of Cr–DNA Adducts at Different Stages of Cr(VI) Reduction. Formation of mutagenic DNA lesions at different time intervals during Cr(VI) reduction was examined by addition of pSP189 DNA for the specified periods of time followed by the immediate purification of the DNA on Bio-Gel P-30 columns. The results showed that the highest levels of mutagenic DNA

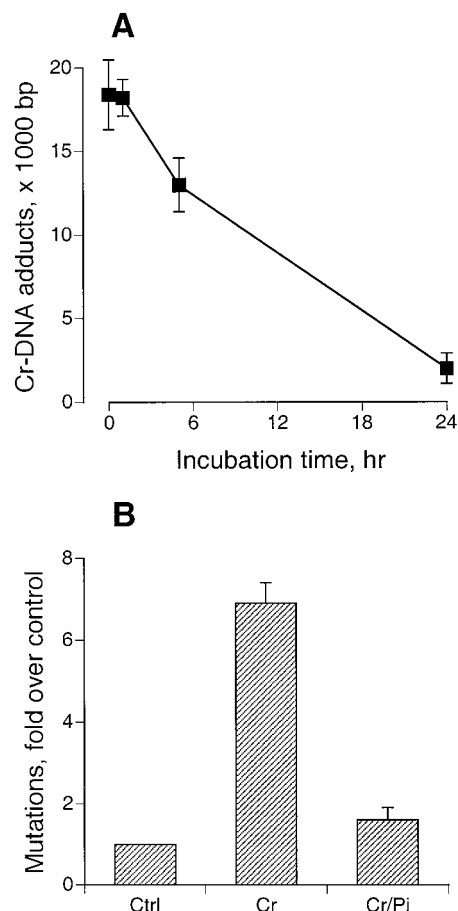


FIGURE 7: Mutagenesis after dissociation of Cr(III) from DNA. Cr–DNA adducts were dissociated by incubation with 50 mM sodium phosphate, pH 7.0, at 37 °C. The initial level of adducts in Cr-treated DNA was 9.2 ± 1.6 Cr/1000 bp. (A) Time-course of Cr removal from DNA in the presence of phosphate buffer. (B) Mutagenic response in control (Ctrl), Cr-treated (Cr), and phosphate-reversed Cr-treated DNA (Cr/Pi). Shown are means \pm SD of six independent experiments.

lesions were formed during 15–30 and 30–60 min time periods (Figure 8, panel A). The extent of mutagenic damage produced at different stages of Cr(VI) reduction clearly did not correspond to the amount of the Cr(VI) reduced. For example, mutagenic damage produced during the first 15 min of reaction was 2.5 times lower in comparison to 30–60 min time interval, whereas approximately 65% Cr(VI) was reduced during 0–15 min and only 15% during 30–60 min (Figure 1). There was no correlation between mutagenic responses and formation of DCFH-oxidizing species at different stages of Cr(VI) reduction (Figure 2, panel A).

Levels of Cr–DNA binding gradually decreased as DNA was added at later stages of Cr(VI) reduction (Figure 8, panel B). The overall trend for the yield of Cr–DNA adduct followed the time-course of Cr(VI) reduction. The largest amount of Cr(VI) was reduced during the first 15 min of the reaction and the highest number of Cr–DNA adducts was formed during this period. However, there was an apparent time-lag between disappearance of Cr(VI) or Cr–(V/IV) (as measured by DCFH oxidation) and Cr–DNA binding, since a decrease in the formation of Cr–DNA adducts was more gradual than the rate of Cr(VI) reduction. Cr–DNA adducts were also formed after the completion of Cr(VI) reduction (after 60 min). The magnitude of mutagenic responses at different periods of Cr(VI) reduction was not

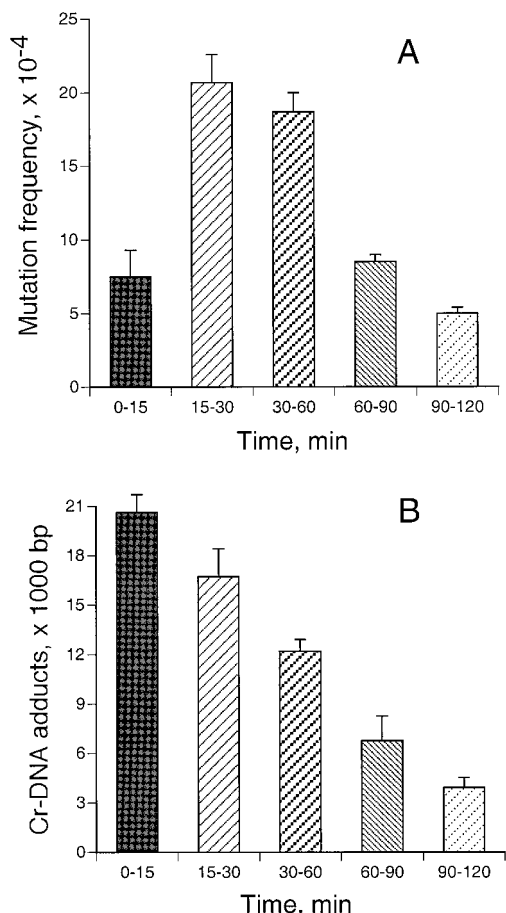


FIGURE 8: Cr–DNA binding and induction of mutagenesis at different intervals after the start of Cr(VI) reduction. Reaction conditions were described in Figure 5. Chromate concentration was 100 μ M. (A) Mutation frequency after subtraction of background values; (B) formation of Cr–DNA adducts. Shown are means \pm SD of four independent experiments.

determined by the overall level of Cr–DNA binding, as evidenced by a low yield of mutants during the first 15 min of Cr(VI) reduction when the highest amount of DNA-bound Cr was found. After the reduction reaction was complete (60–90 and 90–120 min intervals), the yield of mutants was directly related to a number of total Cr–DNA adducts. This result is indicative of the formation of a single class of adducts during postreduction incubations.

Reductive metabolism of Cr(VI) has also been shown to produce Cys–Cr(III)–DNA cross-links (13, 45). Formation of these ternary adducts proceeds through the initial formation of binary Cr(III)–Cys complexes that subsequently bind to DNA (18). On the basis of this mechanism, we reasoned that Cys–DNA cross-linking would follow a time-course distinct from that for the overall Cr–DNA binding. The relative yield of Cys–DNA adducts at different time intervals was indeed different (Figure 9). Only a small fraction of total DNA-bound Cr(III) was involved in the formation of Cys–DNA cross-links at the earliest time interval, whereas later time periods were associated with the progressively higher yields of Cys–DNA adducts. When DNA was added 60 min or later after the start of the reduction reaction, essentially all DNA-bound Cr(III) was involved in the formation of ternary Cys–Cr(III)–DNA adducts. A normalized yield of mutations at late time intervals (predominantly Cys–Cr–DNA cross-links) was 3.6-times higher than that at 0–15

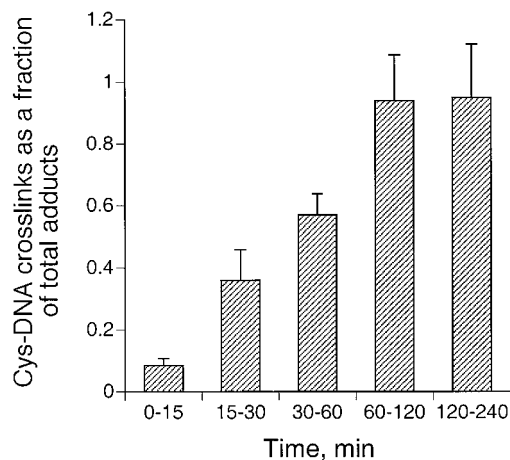


FIGURE 9: Formation of cysteine–DNA cross-links at different time intervals after the start of Cr(VI) reduction. Amount of DNA-bound Cr and cysteine was measured by the inclusion of radiolabeled ⁵¹Cr(VI) and ³⁵S-cysteine, respectively. Excluding incubation time, experimental conditions were as described in Figure 5. MOPS buffer and 200 μ M Cr(VI) were used. Shown are means \pm SD of three independent measurements.

min period (predominantly binary Cr–DNA adducts). After adjustment for the contribution of Cys–DNA adducts to mutagenesis at the 0–15 min period, the mutagenic potential of ternary Cys–Cr(III)–DNA adducts was found to be 5.2-times of that for binary Cr(III)–DNA adducts. The overall mutagenic responses at the specific phases of Cr(VI) reduction were likely determined by both total Cr–DNA binding and the relative amounts of binary and ternary adducts.

Characterization of the supF Mutants. Mutants were collected from treatments of shuttle-vector plasmids with 50 μ M Cr(VI) which gave a 10–15-fold increase in the mutation frequency over background. This ensured that the majority of the mutants (90–95%) were caused by Cr–DNA adducts. The spectrum of spontaneous mutations produced following propagation of the pSP189 plasmids in HF/SV cells has been reported earlier (24). The signature sequence of pSP189 plasmids was used to identify sibling mutants that were not used in the subsequent analysis of mutational changes. Deletions were found in 26% of mutants, among which the majority (10 out of total 13) lost more than 100 bp. Single base substitutions represented the major type of Cr(VI)-induced mutants (Table 1). All point mutations were G:C base pair substitutions. Transversions G:C \rightarrow T:A and transitions G:C \rightarrow A:T accounted for the bulk of all single base substitutions (54 and 34%, respectively). The nature of the adjacent base had a strong influence on the probability of the mutational events at the G:C base pair. Mutations were the most frequent at the sites with another purine located next to the mutated G. The presence of 3' adjacent purine was found in 90%, while 5' purines were present in 71% of single base substitutions. The mutational spectrum did not reveal any strong “hot-spots” for base substitutions along the *supF* gene (Figure 10). The occurrence of mutations along the gene sequence appears to be largely a function of the nature of nucleotides found in the immediate vicinity of G:C pairs. The spectrum of spontaneous mutations is also dominated by the substitutions at the G:C pairs and characterized by a broad distribution along the *supF* sequence with a single “hot-spot” at the position 164 (24).

Table 1: Characterization of Cr-Induced Mutations^a

type of mutations	frequency (%)	base substitutions	frequency (%)
deletions	13 ^b (26)	transitions	
small (<15 bp)	3 (23) ^c	G:C → A:T	14 (34)
large (>100 bp)	10 (77)	A:T → G:C	0 (0)
insertions	2 (3)	transversions	
point mutations (all)	35 (70)	G:C → T:A	22 (54)
single	28 (80) ^c	G:C → C:G	5 (12)
tandem	1 (3)	A:T → T:A	0
multiple	6 (17)	A:T → C:G	0
sequence (3' base effect)	frequency (%)	sequence (5' base effect)	frequency (%)
G*A	25 (61)	AG*	13 (31)
G*G	12 (29)	GG*	16 (40)
G*T	3 (7)	TG*	1 (2)
G*C	1 (3)	CG*	11 (27)
G*Pu	90%	PuG*	71%

^aG*, mutated G base; Pu, purine base. ^bNumber of mutants of the indicated type. ^cPercent of total plasmids.

DISCUSSION

Nature of Premutagenic DNA Lesions Produced during Cr(VI) Reduction by Cysteine. Kinetic studies have suggested two-electron reduction of Cr(VI) by L-Cys as a predominant initial step for the reactions conducted at neutral pH (7, 46). According to the two-electron scheme, the first Cr intermediate would be Cr(IV), not Cr(V) and ERP spectrometry indeed detected only a small signal from Cr(V) (47). The final products of Cr(VI) reduction were L-cystine and Cr(L-cysteinato-N,O,S)₂⁻ (46, 48). Damage by unstable Cr intermediates has been proposed as a potential pathway leading to oxidative DNA damage (22, 23). Extensive oxidation of the redox-sensitive dye DCFH is clearly consistent with the generation of oxidizing species during Cr(VI) metabolism by Cys. Formation of fluorescent DCF has been typically considered to be a result of oxidation reactions generated by hydroxyl radicals or through peroxidase/H₂O₂-dependent mechanisms (49). Cr(V)LDHBA complex has recently been shown to oxidize DCFH directly, demonstrating a role of unstable Cr forms in generation of fluorescent DCF (29). Interestingly, intermediate Cr forms produced in Cr(VI)/Cys reactions were incapable of oxidizing DNA, as shown by the shuttle-vector mutagenesis experiments and electrophoretic analysis of supercoiled plasmids. This result does not necessarily mean that Cr(V) and Cr(IV) produced by other reducers would have similar properties since ligand environment affects reactivity of metal centers. It appears that DCFH is much more sensitive to oxidation in comparison with DNA, and therefore, the formation of fluorescent DCF should not be always regarded as evidence for production of DNA-damaging species.

Induction of mutagenic lesions during Cys-dependent metabolism of Cr(VI) to Cr(III) can be unambiguously attributed to the formation of Cr-DNA adducts. This conclusion is supported by the lack of mutagenic responses when Cr-DNA binding was blocked by the addition of Mg²⁺ ions, phosphate, or EDTA. Furthermore, release of Cr(III) from the plasmid DNA by the phosphate reversal procedure returned mutation frequency to background levels. Oxidative DNA damage is irreversible and mutagenesis derived from oxidative lesions would still be detectable under these conditions. Mutagenic responses were induced at adduct levels that were not overly blocking to replication, as approximately 20–25% transfection efficiency was observed at Cr doses causing a 10–15-fold increase in the mutation frequency. Complete inhibition of Cr-DNA binding by phosphate and EDTA also indicates that DNA-attacking form was most likely Cr(III). Both EDTA and inorganic phosphate form very stable complexes with Cr(III) (41, 50) which would prevent subsequent reactions of the metal with DNA. Although phosphate buffer can remove Cr(III) from DNA, this process is slow and requires at least overnight incubation. EDTA is not very efficient in chelating DNA-bound Cr(III), as evident from the stability of Cr-DNA adducts during agarose electrophoresis in TAE buffer containing 10 mM EDTA. A slow release of Cr(III) implies that the absence of Cr-DNA adducts in reduction reactions conducted in the presence of phosphate or EDTA was a result of sequestration of Cr(III) not of stripping Cr(III) from DNA.

Reduction of Cr(VI) by thiols is typically associated with the generation of thiyl radicals (19, 20). In aerated solutions, the thiyl radicals react with oxygen to produce thiol peroxyl radicals: RS• + O₂ → RSO₂• (51). Thiyl radicals have also been detected during Cr(VI) reduction by glutathione (20) and irradiated solutions containing thiol compounds (52). Shi et al. (19) have found that production of thiyl radicals was the most extensive when the ratio Cys/Cr(VI) was 32:1 and 64:1. Under our conditions, these ratios correspond to approximately 30–60 μM Cr(VI), a dose range that showed strong mutagenic responses. A normal yield of replicated plasmids and the lack of the mutagenic responses in samples lacking Cr(III)-DNA adducts suggests that thiyl radicals/thiol peroxyl radicals are probably not sufficiently reactive to oxidize DNA. This conclusion is also supported by studies on protective effects of various thiols against DNA damage caused by ionizing radiation (52).

Mutagenesis by Cr(III)-DNA Adducts. Formation of premutagenic lesions during different stages of Cr(VI) reduction showed a poor correlation with the overall level of Cr-DNA binding, which appears to be related to a differential formation of binary and ternary Cr-DNA adducts. Cys-Cr(III)-DNA adducts were calculated to be

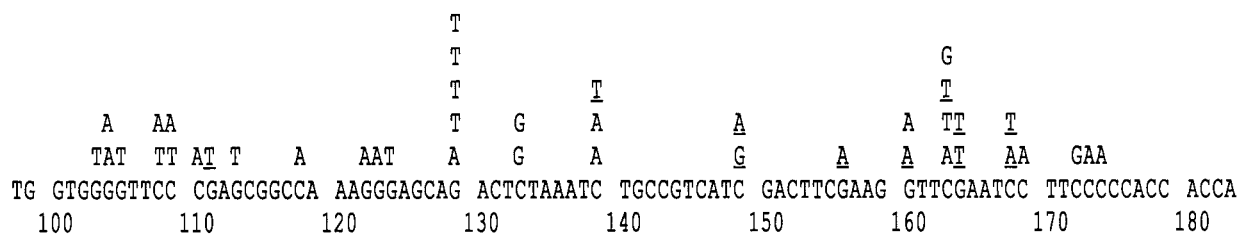


FIGURE 10: Mutational spectrum induced by Cr(VI) in the *supF* gene of pSP189 plasmid. Mutational changes were detected by sequencing. Underlined bases indicate that they originated from clones containing multiple mutations.

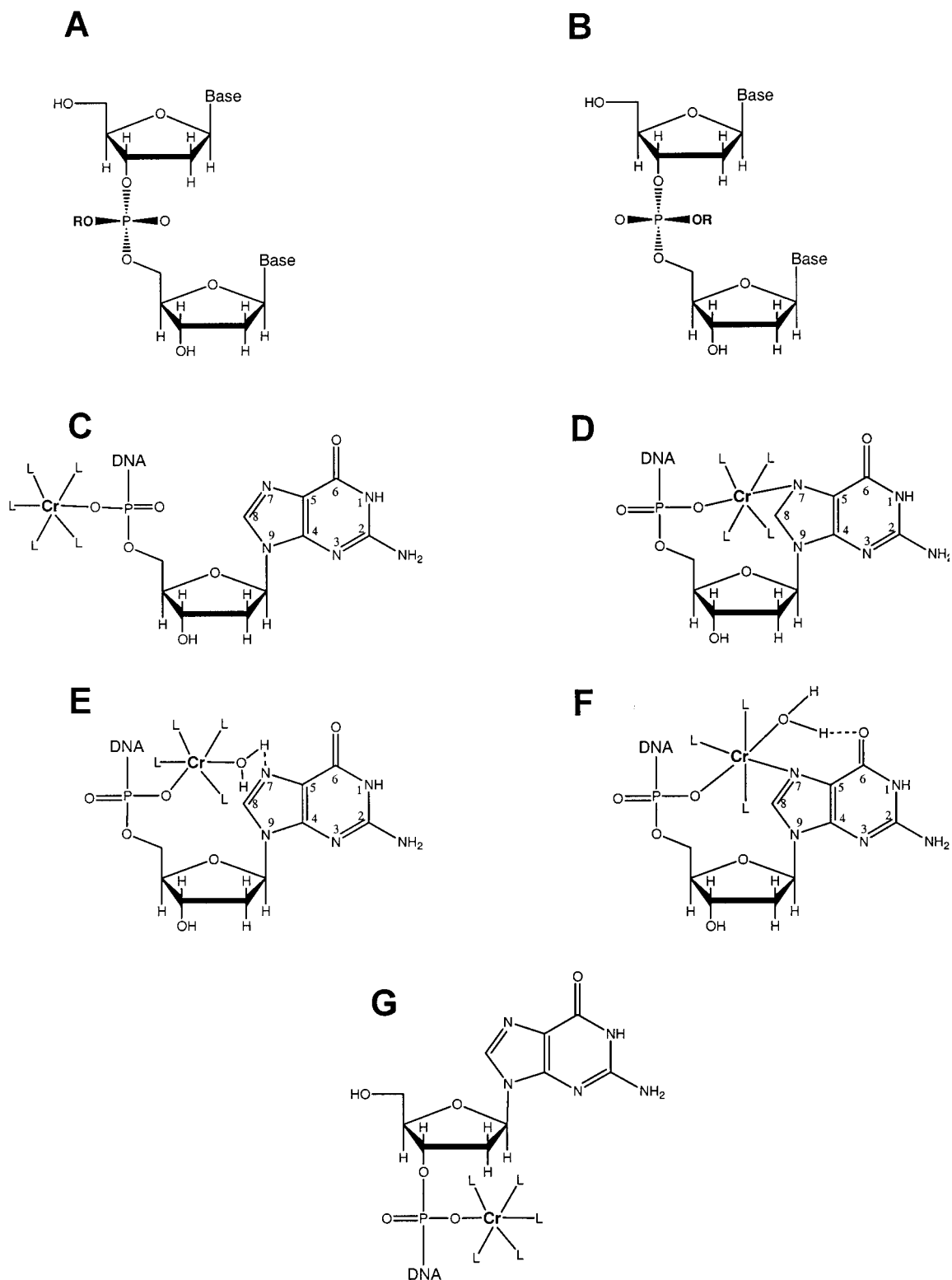


FIGURE 11: Proposed structures of the phosphate-based Cr(III)-DNA adducts. (A) the *S* isomer of DNA alkylphosphotriesters; (B) the *R* isomer of DNA alkylphosphotriesters; (C) Cr(III)-phosphate adduct in the *S* conformation; (D) the *R* isomer of Cr(III)-phosphate adduct stabilized by the direct coordination to N-7 of dG; (E) the *R* isomer of Cr(III)-phosphate adduct stabilized by the hydrogen bonding between coordinated water and N-7 of dG; (F) the *R* isomer of Cr(III)-phosphate adduct stabilized by the direct coordination to N-7 and the hydrogen bonding to O-6 of dG; (G) the *R* isomer formed at 3'-phosphate of dG does not allow additional coordination to N-7. Complexes shown in panels D and E are proposed mutagenic forms of binary Cr(III)-DNA and ternary Cys-Cr(III)-DNA adducts, respectively.

about 4–5 times more mutagenic than binary Cr(III)-DNA complexes. In previous studies, we have found that the mutagenic response was minimal when pSP189 plasmids were modified with $\text{CrCl}_3 \cdot 6\text{H}_2\text{O}$ (24). However, ternary Cys-Cr(III)-DNA adducts produced by reacting DNA with

preincubated Cys/CrCl₃ mixtures induced a much stronger mutagenic response. Mapping of binary and ternary Cr(III)-DNA adducts along the *supF* gene did not reveal base-specificity in the adducts formation or any significant differences in the site-specific distribution of different adducts

(24). The magnitude of mutagenic responses at different phases of Cr(VI) reduction would then appear to be a function of overall Cr–DNA binding and the ratio of ternary to binary adducts.

Extrapolation of total Cr–DNA adducts to 20 Cr atoms/plasmid gives a mutation frequency of 30×10^{-4} (6.5-fold increase over control). Formation of the same number of adducts with benzo[*a*]pyrene 7,8-diol-9,10-epoxide, 1-nitrosopyrene, *N*-acetoxy-2-acetylaminofluorene, or trifluoro-derivative of *N*-acetoxy-2-acetylaminofluorene resulted in 40×10^{-4} (28.6-fold), 11.6×10^{-4} (8.3-fold), 12×10^{-4} (8.6-fold), and 10×10^{-4} (7.1-fold increase) mutation frequencies, respectively (53–55). Thus, it appears that mutagenic potency of total Cr(III)–DNA adducts (binary and ternary complexes combined) was comparable to that of bulky adducts formed at C-8 position of G (1-nitrosopyrene, *N*-acetoxy-2-acetylaminofluorene, or its trifluoro-derivative). An average frequency of conversion of a Cr-modified site into mutation was about 1 per 50 adducts. Base substitutions produced by Cr(III)–DNA complexes targeted G/C pairs resulting in predominantly G/C → T/A and G/C → A/T changes. This correlates well with mutational changes generated by Cr(VI) exposure of human lymphoblastoid cells in which G/C → T/A and G/C → A/T substitutions were most frequently observed (11). Distribution of mutations induced by Cr(VI) was very different from the mutational spectrum produced by H₂O₂.

Cr³⁺ ions are hard Lewis acids strongly preferring O atoms as compared to S (50). Charged oxygen groups are also better ligands as compared to N atoms. In mononucleotides and DNA, this preference for O[−] ligands leads to the formation of inner sphere complexes of Cr(III) with phosphates (17, 18, 43, 56, 57). Phosphate-bound 3d metals typically exhibit some interaction with N-7 of purine bases (58). This interaction is approximately 10-times stronger for GMP as compared to AMP, and it is caused by a greater basicity of N-7 of GMP. The extent of microchelate formation varies depending on the degree of the softness of the metal and may involve either direct coordination to N-7 or outer-sphere binding. Inner-sphere coordination of Cr(III) to TMP, CMP, or AMP was found to be exclusively to the phosphate group (56), but additional base coordination was detected in some binary Cr(III)–GMP complexes (43). In addition to N-7, a potential Cr(III)–GMP interaction can also occur at O-6 through hydrogen binding with coordinated water. A direct N-7/O-6 chelate is unlikely because the angle (C-6)–(C-5)–(N-7) is 132° (59), which is too wide to be accommodated into the octahedral geometry of Cr(III) complexes. Ternary Cr(III)–mononucleotide complexes with amino acids obtained through different synthetic approaches were always formed by inner-sphere coordination to phosphate oxygen (17, 18). Various modes of Cr(III) coordination with DNA are graphically presented in Figure 11.

Alkylation of the phosphodiester group results in adducts that can have either an *R* or *S* configuration (60). The *S* isomer would feature Cr(III) atom pointing away from the DNA helix, whereas the *R* isomer points metal toward the major groove (Figure 11, panels A and B). Cr(III)–Cys complex is a relatively bulky structure and a ternary adduct would seem more likely to be formed in the *S* configuration due to steric considerations. However, additional Cr(III) interactions with N7-G (and possibly, O6-G) may lead to a

preferential formation of Cys–Cr–DNA adducts in the *R* conformation at the phosphodiester group located in the 5′ position to G (Figure 11, panels F and E). The *R* isomer of alkylphosphotriesters has been found to alter DNA structure to a much greater extent than its *S* counterpart (61–63). Positioning of Cys ligand in the close vicinity to DNA could force it to be partially inserted into the DNA helix. Structural distortions caused by this type of DNA binding would likely include base unstacking, and this suggestion is supported by diminished binding of ethidium bromide to Cr-modified DNA. Coordination of Cr(III) to N7-G per se does not seem to be important in mutagenesis since binary Cr–DNA adducts are weakly mutagenic (24 and this study). Another factor influencing DNA structure at the sites of Cr(III) binding includes neutralization of the negative charge on the phosphate, which could lead to altered interactions with DNA polymerase and increased propensity to bending (64). Base unstacking has also been reported for oligonucleotides containing methyl-, ethyl-, or isopropylphosphotriesters (62, 65, 66). Modifications with the bulkier alkyl group led to larger changes in oligonucleotides, and the structure of GpA and ApA oligonucleotides was more perturbed as compared to ApT or TpT (62, 65–67). These findings are consistent with a higher mutagenicity of bulky Cys–Cr(III)–DNA adducts and the observed preference for positions flanked by A. Additional factors contributing to a site-specific distribution of mutations could involve variable rates of adduct removal at different positions (68) and sensitivity of DNA polymerase to structural distortions in different sequence context (69). The DNA chain elongation of isopropyl phosphotriester-containing oligonucleotides has been shown to be strongly influenced by the base in the 5′ position (70). Interestingly, only the *S* isomer of methylphosphotriesters is removed in *E. coli* cells leaving a more structure-disturbing *R* isomer unrepaired (71). If a similar preference in repair of the *S* isomers exists in human cells, it may lead to a higher frequency of mutational events at the sites favoring formation of phosphotriester adducts in the *R* conformation.

REFERENCES

- IARC. (1990) IARC monographs on the evaluation of carcinogenic risks to humans. *Chromium, Nickel and Welding*. Vol. 49, pp 49–256, World Health Organization, Lyon, France.
- Langardt, S. (1990) *Am. J. Ind. Med.* 17, 189–215.
- Sorahan, T., Burges, D. C., Hamilton, L., and Harrington, J. M. (1998) *Occup. Environ. Med.* 55, 236–242.
- Agency for Toxic Substances and Disease Registry. (1993) *Toxicological Profile for Chromium*. Washington, DC, Department of Health and Human Services.
- Connett, P., and Wetterhahn, K. E. (1983) *Struct. Bonding* 54, 93–124.
- Suzuki, Y., and Fukuda, K. (1990) *Arch. Toxicol.* 64, 169–176.
- O'Brien, P., Wang, G., and Wyatt, P. B. (1992) *Polyhedron* 24, 3211–3216.
- Sen, P., Conway, K., and Costa, M. (1987) *Cancer Res.* 47, 2142–2147.
- Biedermann, K. A., and Landolph, J. R. (1990) *Cancer Res.* 50, 7835–7842.
- Snow, E. (1992) *Pharmacol. Ther.* 53, 31–65.
- Chen, J., and Thilly, W. G. (1994) *Mutat. Res.* 323, 21–27.
- Wise, J. P., Stearns, D. M., Wetterhahn, K. E., and Patierno, S. R. (1994) *Carcinogenesis* 15, 2249–2254.
- Zhitkovich, A., Voitkun, V., and Costa, M. (1995) *Carcinogenesis* 16, 907–913.
- Costa, M. (1990) *J. Cell Biochem.* 92, 127–135.

15. Xu, J., Bublely G. J., Detrick B., Blankenship L. J., and Patierno, S. R. (1996) *Carcinogenesis* 17, 1511–1517.
16. Zhitkovich, A., Voitkun, V., Kluz, T., and Costa, M. (1998) *Environ. Health Perspect.* 106 (Suppl. 4), 969–974.
17. Vicens, M., Fiol, J. J., Terron, A. (1989) *Inorg. Chim. Acta* 157, 127–132.
18. Zhitkovich, A., Voitkun, V., and Costa, M. (1996) *Biochemistry* 35, 7275–7282.
19. Shi, X., Dong, Z., Dalal, N. S., Gannett, P. M. (1994) *Biochim. Biophys. Acta* 1226, 65–72.
20. Aiyar, J., Berkovits, H. J., Floyd, R. A., and Wetterhahn, K. E. (1990) *Chem. Res. Toxicol.* 3, 595–603.
21. Stearns, D. M., and Wetterhahn, K. E. (1994) *Chem. Res. Toxicol.* 7, 219–230.
22. Levina, A., Barr-David, G., Codd, R., Lay, P., Dixon, N. E., Hammershoi, A., and Hendry, P. (1999) *Chem. Res. Toxicol.* 12, 371–381.
23. Sugden, K. D., and Wetterhahn, K. E. (1997) *Chem. Res. Toxicol.* 10, 1397–1406.
24. Voitkun, V., Zhitkovich, A., and Costa, M. (1998) *Nucleic Acids Res.* 26, 2024–2030.
25. Earley, J. E., and Cannon, R. D. (1965) in *Transition Metal Chemistry* (Carlin, R. L., Ed.) Vol.1, pp 33–109, Marcel Dekker, NY.
26. Capellmann, M., Mikalsen, A., Hindrum, M., and Alexander, J. (1995) *Carcinogenesis* 16, 1135–1139.
27. Yuann, J. M., Liu, K. J., Hamilton, J. W., and Wetterhahn, K. E. (1999) *Carcinogenesis* 20, 1267–1275.
28. Standeven, A. M., and Wetterhahn K. E. (1992) *Carcinogenesis* 13, 1319–1324.
29. Martin, B. D., Schoenfeld, J. A., and Sugden, K. D. (1998) *Chem. Res. Toxicol.* 11, 1402–1410.
30. Zhitkovich A., Shrager S., and Messer, J. (2000) *Chem. Res. Toxicol.* 13, 1114–1124.
31. Parris, C. N., and Seidman, M. M. (1992) *Gene* 117, 1–5.
32. Ariza, R. R., Roldan-Arjona, T., Hera, C., and Pueyo, C. (1993) *Carcinogenesis* 14, 303–305.
33. Hanahan, D., Jessee, J., and Bloom, F. R. (1991) *Methods Enzymol.* 204, 83–88.
34. Jeong, J. K., Wogan, G. N., Lau, S. S., and Monks, T. J. (1999) *Cancer Res.* 59, 3641–3645.
35. Brabec, V., Kasparkova, J., Vrana, O., Novakova, O., Cox, J. W., Qu, Y., and Farrel, N. (1999) *Biochemistry* 38, 6781–6790.
36. Kasparkova, J., Novakova, O., Vrana, O., Farrel, N., and Brabec, V. (1999) *Biochemistry* 38, 10997–10005.
37. Cohen, G. L., Bauer, W. R., Barton, J. K., and Lippard, S. J. (1979) *Science* 203, 1014–1016.
38. Sip, M., Schawarz, F., Vovelle, F., Ptak, M., and Leng, M. (1992) *Biochemistry* 31, 2508–2513.
39. Bradley, A. J., Yarema, K. J., Lippard, S. J., and Essigmann, J. M. (1993) *Biochemistry* 32, 982–988.
40. Yarema, K. J., Wilson, J. M., Lippard, S. J., and Essigmann, J. M. (1994) *J. Mol. Biol.* 236, 1034–1048.
41. Gerdorn, L. E., Baenzinger N. A., and Goff, H. M. (1981) *Inorg. Chem.* 20, 1606–1609.
42. Sander, C., and Ts'o, P. O. P. (1971) *J. Mol. Biol.* 55, 1–21.
43. Calafat, A. M., Mulet, D., Fiol, J. J., Terron, A. (1987) *Inorg. Chim. Acta* 138, 105–112.
44. Montrel', M. M., Shabarchina, L. I., Pletneva, T. V., and Ershov, Iu. A. (1993) *Biofizika* 38, 636–643.
45. Voitkun, V., Zhitkovich, A., and Costa, M. (1994) *Environ. Health Perspect.* 102 (Suppl. 3), 251–255.
46. Kwong, D. W. J., and Pennington, D. E. (1984) *Inorg. Chem.* 23, 2528–2532.
47. Kitagawa, S., Seki, H., Kametani, F., and Sakurai, H. (1988) *Inorg. Chim. Acta* 152, 251–255.
48. Kaiwar, S. P., Sreedhara, A., Raghavan, M. S. S., and Rao, C. P. (1996) *Polyhedron* 15, 765–774.
49. LeBel, C. P., Ischiropoulos, H., and Bondy, S. C. (1992) *Chem. Res. Toxicol.* 5, 227–231.
50. Larkworthy, L. F., Nolan, K. B., and O'Brien, P. (1988) in *Comprehensive Coordination Chemistry* (Wilkinson, G., Ed.) Vol. 3, pp 699–969, Pergamon Press, New York.
51. Tamba, M., Simone, G., and Quitiliani, M. (1986) *Int. J. Radiat. Biol.* 50, 595–600.
52. Lafleur, M. V. M., and Retel, J. (1993) *Mutat. Res.* 295, 1–10.
53. Yang, J.-A., Maher, V. M., and McCormick, J. J. (1987) *Proc. Natl. Acad. Sci.* 84, 3787–3791.
54. Yang, J.-A., Maher, V. M., and McCormick, J. J. (1988) *Mol. Cell. Biol.* 8, 3364–3372.
55. Maher, V. M., Yang, J.-L., Mah, C.-M., and McCormic, J. J. (1989) *Mutat. Res.* 220, 83–92.
56. Fiol, J. J., Terron, A., and Moreno, V. (1984) *Inorg. Chim. Acta* 83, 69–73.
57. Calafat, A. M., Fiol, J. J., Terron, A. (1990) *Inorg. Chim. Acta* 169, 133–139.
58. Sigel, H., Massoud, S. S., and Corfu, N. A. (1994) *J. Am. Chem. Soc.* 116, 2958–2971.
59. Frommer, G., Preut, H., Lippert, B. (1992) *Inorg. Chim. Acta* 193, 111–117.
60. Swenson, D. H., and Lawley, P. D. (1978) *Biochem. J.* 171, 575–587.
61. Summers, M. F., Powell, C., Egan, W., Byrd, R. A., Wilson, W. D., Zon, G. (1986) *Nucleic Acids Res.* 14, 7421–7436.
62. Lawrence D. P., Wenqiao, C., Zon, G., Stec, W. J., Uznanski, B., and Broido, MS. (1987) *J. Biomol. Struct. Dynam.* 4, 757–783.
63. Broido, M. S., and Mezei, M. (1990) *Biopolymers* 29, 597–607.
64. Strauss-Soukup, J. K., Vaghefi, M. M., Hogrefe, R. I., Maher, L. J., 3rd (1997) *Biochemistry* 36, 8692–8698.
65. Miller, P. S., Fang, K. N., Kondo, N. S., and Ts'o, P. O. P. (1971) *J. Am. Chem. Soc.* 93, 6657–6665.
66. Kan, L. S., Cheng, D. M., Chandrasegaran, S., Pramanik, P., and Miller, P. S. (1987) *J. Biomol. Struct. Dynam.* 4, 785–796.
67. Weinfeld, M., and Livingston, D. C. (1986) *Biochemistry* 25, 5083–5091.
68. Tornaletti S., and Pfeifer G. P. (1994) *Science* 263, 1436–1438.
69. Litinski, V., Chenna, A., Sagi, J., and Singer, B. (1997) *Carcinogenesis* 18, 1609–1615.
70. Yashiki, T., Yamana, K., Nunota, K., and Negishi, K. (1992) *Nucleic Acids Symp. Ser.* 27, 197–198.
71. Myers, L. C., Terranova, M. P., Ferentz, A. E., Wagner, G., Verdine, G. L. (1993) *Science* 261, 1164–1167.

BI0015459